ADVANCED FUNCTIONAL MATERIALS
www.afm-journal.de

Silk Hydrogels as Soft Substrates for Neural Tissue Engineering

*Amy M. Hopkins, Laura De Laporte, Federico Tortelli, Elise Spedden, Cristian Staii, Timothy J. Atherton, Jeffrey A. Hubbell, and David L. Kaplan**

There is great need for soft biomaterials that match the stiffness of human tissues for tissue engineering and regeneration. Hydrogels are frequently employed for extracellular matrix functionalization and to provide appropriate mechanical cues. It is challenging, however, to achieve structural integrity and retain bioactive molecules in hydrogels for complex tissue formation that may take months to develop. This work aims to investigate mechanical and biochemical characteristics of silk hydrogels for soft tissue engineering, specifically for the nervous system. The stiffness of 1 to 8% silk hydrogels, measured by atomic force microscopy, is 4 to 33 kPa. The structural integrity of silk gels is maintained throughout embryonic chick dorsal root ganglion (cDRG) explant culture over 4 days whereas fibrin and collagen gels decrease in mass over time. Neurite extension of cDRGs cultured on 2 and 4% silk hydrogels exhibit greater growth than softer or stiffer gels. Silk hydrogels release <5% of neurotrophin-3 (NT-3) over 2 weeks and 11-day old gels show maintenance of growth factor bioactivity. Finally, fibronectin- and NT-3-functionalized silk gels elicit increased axonal bundling suggesting their use in bridging nerve injuries. These results support silk hydrogels as soft and sustainable biomaterials for neural tissue engineering.

1. Introduction

Spinal cord and traumatic brain injuries (TBI) are sustained by millions of people each year, with almost half a million emergency department visits for TBI made annually by children.[1] Research efforts toward neural tissue engineering are in the early stages of discovery, with investigations of regeneration of central nervous system (CNS) tissues,[2,3] soft biomaterials to decrease inflammation from implantable devices,[4–7] and non-invasive drug delivery to the CNS.[6,8–10] Previous efforts to develop biomaterials for neural tissue repair have focused on anti-inflammatory coatings for implantable devices[10–13] or construction of nerve guide conduits for peripheral and central nerve repair.[14–22] With increased focus on advanced, three-dimensional biomaterial systems, progress is being made toward the engineering of soft neural tissues *ex vivo* for modeling and implantation.

It is evident that substrate stiffness significantly affects cell attachment, survival, and growth and therefore should be taken into consideration when engineering scaffolds for neural cell culture. Traditionally, neuronal cells cultured in vitro are plated on laminin (LN)-, fibronectin (FN)-, poly-lysine-coated glass or tissue culture plastic (TCP) providing integrin binding sites for cell attachment and neurite extension.[23–26] Neural tissues are inherently soft, with stiffness values generally less than 100 kPa (ranging from <1 kPa for brain slices[27] and single brain cells[28] to ≈90–230 kPa for spinal cord,[29,30] as compared to ≈70 GPa for glass). This has prompted studies of neural cell growth and function on substrates of varying stiffness. For example, Koch et al. found that peripheral nerve outgrowth is more sensitive to changes in substrate stiffness as compared to CNS hippocampal neural extension.[31] This is perhaps due to the increased diversity in mechanical and biochemical environment of peripheral nervous system extracellular matrices (ECMs) versus those of the CNS, where connective tissue consists mostly of glial cells.[31] There is also evidence that effects of substrate stiffness on neuron extension and differentiation vary with the presence of particular ECM molecules and enzyme expression.[32]

In addition, biochemical cues are integral to reconstruction of neural tissue in vitro, specifically for nerve growth guidance toward the target effector without collateral sprouting. Many groups have reported on the soluble and contact-mediated ECM factors responsible for axonal guidance including both haptotactic cues (i.e. collagen, LN, FN, and cell adhesion molecules) and chemotactic cues (i.e. neurotrophic factors).[33–37] However,

A. M. Hopkins, Prof. D. L. Kaplan
Department of Biomedical Engineering
Tufts University
Medford, MA 02155, USA
E-mail: david.kaplan@tufts.edu
A. M. Hopkins, Dr. L. De Laporte, Dr. F. Tortelli
Prof. J. A. Hubbell
Institute of Bioengineering
School of Life Sciences and Institute for
Chemical Sciences and Engineering, School of Basic Sciences
École Polytechnique Fédérale de Lausanne (EPFL)
1015 Lausanne, Switzerland
E. Spedden, Prof. C. Staii, Prof. T. J. Atherton
Department of Physics and Astronomy
and Center for Nanoscopic Physics
Tufts University
Medford, MA 02155, USA

DOI: 10.1002/adfm.201300435

the mechanisms of axonal bundling (fasciculation) during development and for directed, long distance nerve regeneration are still being elucidated.

The current study employs NT-3 to stimulate neurite outgrowth due to its known neurotrophic potency in sensory and motor neurons,[38] as well as FN, which plays a major role in cell adhesion, growth, migration, and wound healing. FN is well documented in terms of structure and function of peptide fragments important for cell adhesion (RGD, PHSRN, $III_{9\text{-}10}$),[39] growth factor binding ($III_{12\text{-}14}$),[40] and axonal outgrowth promotion (GFGDS).[41] Notably, FN $III_{12–14}$ binds NT-3 with high affinity, displaying a K_d of 1.5 nM and a K_{off} of only $6.2 \times 10^{-4} s^{-1}$.[40] We hypothesize that these attributes of FN play an important role in augmenting neurite extension during neural regeneration in FN-functionalized silk hydrogels.

To investigate the roles of microenvironmental stiffness and ECM composition on axonal extension for neural tissue engineering and regeneration, a systematic approach to the design of soft substrates is required. Hydrogels are crosslinked polymer networks comprised of over 99% liquid (water), comparable to the fibrous protein network of natural ECMs, and are often used as soft substrates in tissue engineering. Synthetic materials including polydimethylsiloxane (PDMS)[42] and polyacrylamide hydrogels[31,43,44] are frequently employed as soft substrates for cell culture since their stiffness is directly related to extent of chemical crosslinking. Here, we sought materials of controllable biomechanics that could be formed under non-toxic conditions. Although polyethylene glycol (PEG) hydrogels are frequently suggested for cell encapsulation and are non-toxic, it has been found that neuronal cell cultures in PEG hydrogels experienced initial cell death within 1 day of culture and did not exhibit greater viability or proliferation as compared to monolayer controls, even when supplemented with soluble growth factors.[45] Natural biomaterials that have been explored for neural cell culture include collagen,[46] Matrigel,[2] alginate,[47] agarose,[48] and fibrin.[49] Although suitable for 3D cell culture in vitro, these hydrogels are known to exhibit fast release of loaded growth factors and degrade very quickly often not allowing adequate time for cell attachment, growth, and tissue assembly for tissue engineering applications.

Silk fibroin is a natural biomaterial that is extracted from the cocoons of the *Bombyx mori* silkworm. It is non-immunogenic[50,51] and has been used clinically in sutures for decades. Aqueous silk solutions can be obtained through water-based processing of the solid fibers and is used in the construction of a myriad of biomaterial scaffolds ranging from films to electrospun mats to hydrogels.[52] Silk fibroin hydrogels form through physical crosslinking of large hydrophobic blocks of amino acids forming β-sheets when activated by environmental changes such as shear stress (i.e. sonication or vortexing), lower pH, higher temperature, and changes in osmolarity.[53–55] Recently, silk hydrogels have been employed for the delivery of small molecules and proteins[56] as well as cell encapsulation.[57] Silk is known for its impressive mechanical strength and confined compression testing of silk gels has revealed bulk mechanical properties within physiological range for soft tissues.[58] Additionally, silk hydrogels degrade much more slowly than other hydrogel systems (i.e. on the order of months[57] vs. weeks)[59–61] making it a highly attractive scaffold for long-term tissue engineered constructs and *in vivo* applications.

The goals of the current study were to investigate silk hydrogels' mechanical and biochemical properties as indicated by cDRG neurite outgrowth, as well as the development of silk-based soft biomaterials with controllable stiffness and ECM composition, long-term stability, and bioactivity for neural tissue engineering. Further experimentation of silk hydrogels as an ECM through functionalization with FN led to observations of differences in neurite outgrowth and fasciculation. These results provide new knowledge of mechanical properties of silk hydrogels as measured by atomic force microscopy (AFM) indentation, functionalization of silk gels with growth factors and ECM molecules, and facilitation of neurite extension by low stiffness of silk substrates.

2. Results

2.1. Stiffness and Structural Integrity of Silk Hydrogels

AFM-based force mapping was performed on 1, 2, 4, and 8% w/v silk hydrogels to obtain mean elastic (Young's) modulus measurements of 4.8, 7.4, 22.4, and 33.1 kPa, respectively (**Figure 1**a). These elastic modulus values are comparable to those of neural tissues as well as other hydrogels such as fibrin, agarose, and collagen (Figure 1b, **Table 1**).

To test the integrity and maintenance of the volume and shape of silk hydrogels for long-term cultures, hydrogels were cast in 96-well plates and incubated in phosphate buffered saline (PBS) for 2 weeks. While silk hydrogels maintained shape and hydration, fibrin and collagen gels lost integrity and began to break down even in the absence of exogenous proteases (**Figure 2**a). Fast degradation of fibrin and collagen

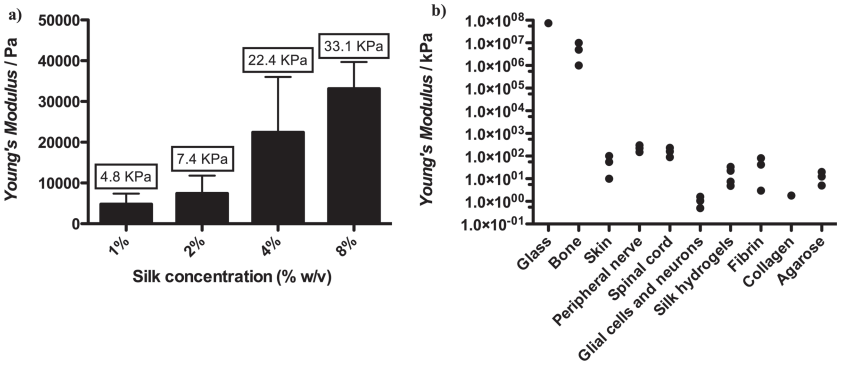

Figure 1. a) Stiffness measurements of silk hydrogels. AFM force mapping of silk hydrogels casted on glass yielded mean Young's modulus values of 4.8, 7.4, 22.4, and 33.1 kPa for 1, 2, 4, and 8% w/v silk, respectively. Error bars represent one standard deviation. b) Summary of stiffness of various tissues and cell culture substrates from Table 1.

Table 1. Range of stiffness of tissues and cell culture substrates

Tissue/ substrate	Stiffness [kPa]	References
Glass	7.4×10^6	[62]
Bone	10^6-10^7	[63]
Skin	10–100	[64]
Peripheral nerves	150–300	[65]
Spinal cord	≈90–230	[29,30]
Glial cells and neurons	≈0.5–1.6	[28,27]
Silk hydrogels	≈4.8–400	[58]
Fibrin gel	≈3–80	[49]
Collagen	≈1.8	[66]
Agarose	≈5–20	[67]

gels as compared to silk hydrogels was also observed during cDRG culture as seen by the formation of holes (white arrows) in 4-day-old cDRG cultures on fibrin and collagen (Figure 2b). Gel degradation rate was quantified as mass loss during α-chymotrypsin degradation (Figure 2c). Fibrin degraded completely by day 6 and only 17% collagen by mass remained on day 12 whereas over 50% of both 2 and 4% silk gels remained at 24 days (Figure 2c).

2.2. cDRG Neurite Extension on Silk Hydrogels of Different Stiffness

cDRGs are commonly employed as a model of peripheral nerve extension and regeneration and were chosen for the presented experiments due to their relevance in the field[68–76] and ease of isolation and culture. cDRGs cultured on 2% and 4% silk hydrogels elicited the greatest neurite extension and density at each time point (**Figure 3**a,b) with maximum neurite extension of ≈1500 μm and a density of ≈47% as compared to ≈400 μm length and ≈10% density of neurites grown on collagen gel. The highest overall growth rates were observed on the 2% and 4% silk hydrogels with the greatest rate of extension 303 μm day^{-1} on 2% silk hydrogels (vs. 87 μm day^{-1} on collagen) and the greatest rate of increase in neurite density 11.5% day^{-1} (vs. 1.8% day^{-1} on collagen) (Figure 3a,b).

2.3. Long-Term Bioactivity of NT-3-Loaded Silk Hydrogels

Growth factors loaded into hydrogels should maintain bioactivity in order to sustain long-term cultures and tissue regeneration. Silk gels loaded with 40 ng mL^{-1} NT-3 and incubated in cell culture media for 11 days prior to cDRG culture elicited the same length and density neurite extension as silk gels incubated for 1 day (**Figure 4**a,b). Furthermore, surface detection of NT-3 bound to silk hydrogels showed silk concentration-dependent binding as well as greater overall binding to silk gels as compared to TCP and fibrin gel (Figure 4c).

2.4. Release of NT-3 from Silk Hydrogels

Release studies were conducted to understand the efficacy of silk hydrogels as functionalized ECM substrates for neural cell culture. The release of NT-3 from silk hydrogels with and without FN was quantified using enzyme-linked immunosorbent assay

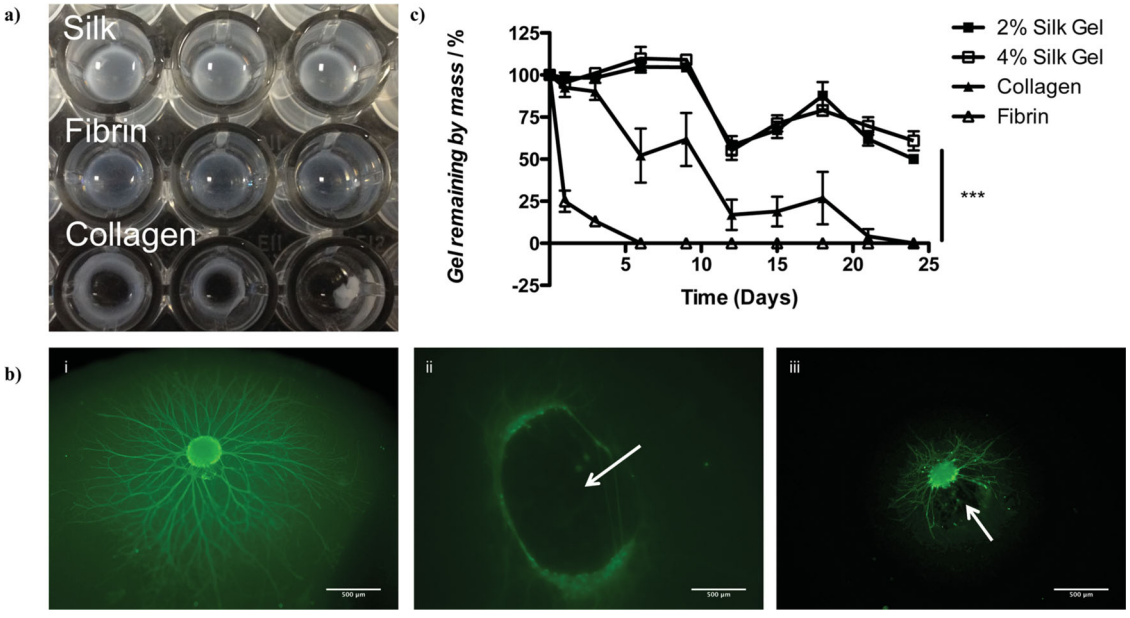

Figure 2. Integrity of silk hydrogels. a) Images of silk, fibrin, and collagen hydrogels after 2 weeks incubation at 37 °C in PBS. b) Immunofluorescent (β-tubulin III) images of day in vitro 4 cDRGs cultured on silk (i), fibrin (ii), and collagen (iii) hydrogels with white arrows identifying holes in gels. c) α-chymotrypsin degradation of silk hydrogel compared to collagen and fibrin. Error represented as standard error mean, *** = $p < 0.0001$ by day 21. Green = β-III tubulin, scale bars = 500 μm.

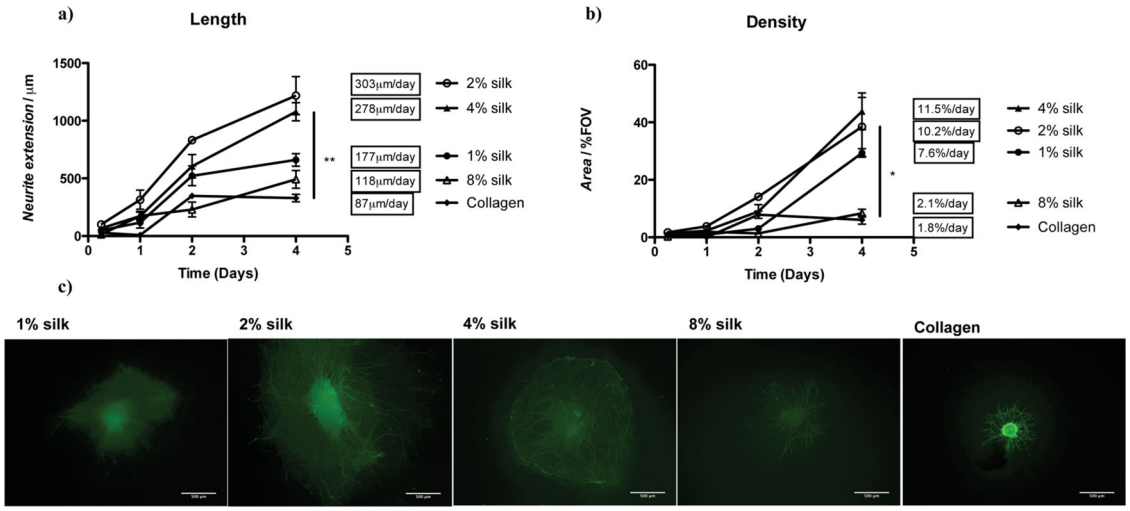

Figure 3. Rate of cDRG neurite extension on hydrogels of different stiffness. a,b) Growth rates of a) length and b) density of neurite extensions of cDRGs cultured for 6 h and 1, 2, and 4 days on 1, 2, 4, and 8% silk hydrogels, and collagen. Significance determined by t-test of 2% silk and collagen at day 4. $^{**}p < 0.01$, $^{*}p < 0.05$. c) Immunofluorescent (β-tubulin III) images of representative cDRGs cultured on silk and collagen hydrogels at day 4 in vitro. FOV = field of view, scale bars = 500 μm.

(ELISA) (**Figure 5**). Less than 5% of loaded NT-3 was released over 25 days and appeared to level off after 2 weeks in agreement with recent long-term release studies of bioactive proteins from sonicated silk hydrogels.[56,77] The addition of FN significantly decreased NT-3 release from the silk gels.

2.5. cDRG Neurite Extension on Functionalized Silk Hydrogels

To explore responses in neurite extension to changes in the ECM functionalization of the silk hydrogels, 4% silk gels were loaded with 40 ng mL^{-1} NT-3 with or without 10 nM FN or LN.

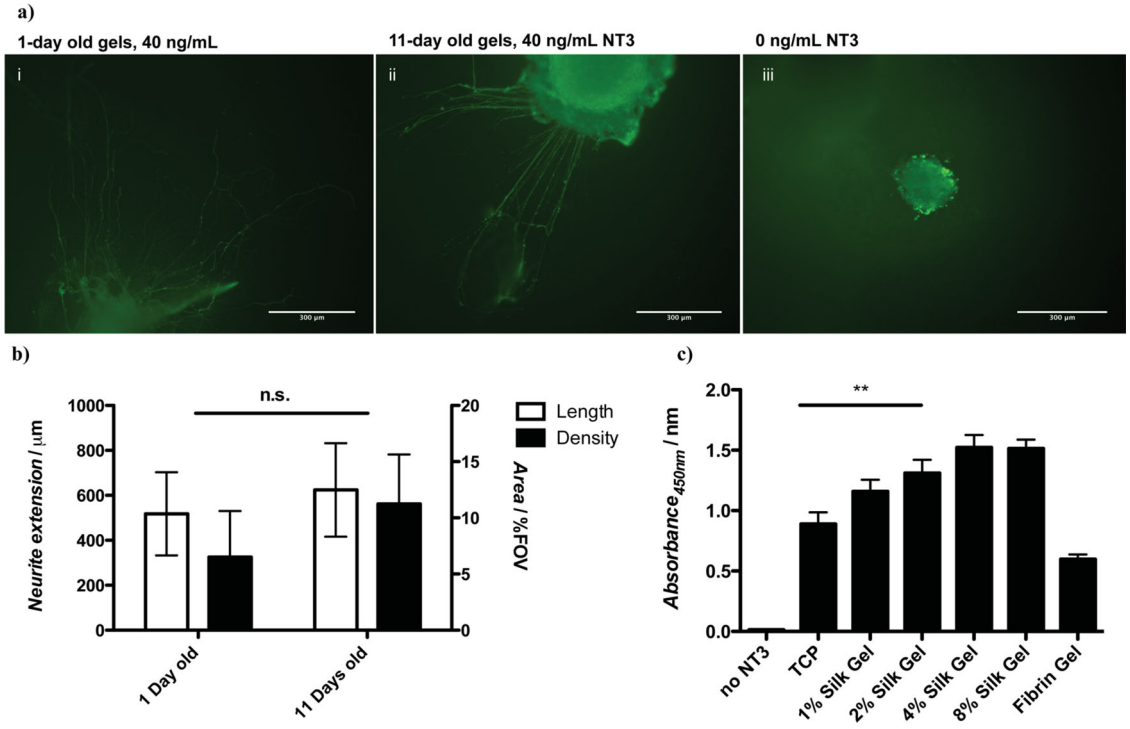

Figure 4. Long-term bioactivity of silk hydrogels. a) Immunofluorescent images of cDRG neurite extension on 4% silk hydrogels loaded with 40 ng mL^{-1} NT-3 and incubated for 1 (i) and 11 (ii) days in media as compared to those cultured on silk gels without NT-3 (iii). Day 4 in vitro, green = β-tubulin III. b) Quantification of neurite length and density of cDRGs cultured on silk hydrogels in (a). c) Antibody detection of NT-3 bound to silk hydrogels as compared to negative control (no NT-3), TCP, and fibrin gel. Error bars represent standard error of the mean, $^{**}p < 0.01$. Scale bars = 300 μm.

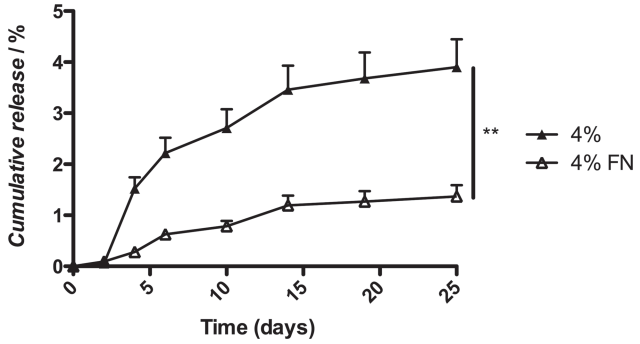

Figure 5. ELISA quantification of cumulative release of NT-3 from 4% silk hydrogels over 25 days with and without FN. **p < 0.01.

Although literature suggests that FN decreases neurite extension,[78] we found that FN-functionalized silk gels produced cDRG extensions longer than those cultured on substrates functionalized with LN and NT-3, perhaps due to FN's integrin and growth factor binding sites acting synergistically with NT-3 (**Figure 6**a). The extent of fasciculation as a function of distance from the explant body was quantified using an orientational distribution function (ODF) that assessed extent of alignment of neurites with a radially aligned vector field.[79] We found ECM-functionalized silk hydrogels exhibited greater fasciculation of neurites as compared to silk hydrogel alone with NT-3 (Figure 6b,c). Summated (Figure 6b,c, top) and radially resolved (Figure 6b,c, bottom) histograms show that a greater number of tangent vectors were in the radial direction (angle = 0) in images of cDRGs cultured on silk hydrogels functionalized with FN as compared to those without. Quantification by Fourier series expansion of the ODF showed a lesser extent of radial outgrowth of neurites on silk gels without (0.152) versus those with (0.281) FN (Figure 6b,c, top). Furthermore, examination of spatially resolved orientational distributions of neurite outgrowth shows a high degree of radially aligned outgrowth close to the explant body in both conditions (0.328 and 0.281), but a significant decrease in radial outgrowth with increasing distance from the explant body in the absence of FN (Figure 6b). The extent of radially aligned outgrowth in the condition with FN, however, gradually increased with increased distance from the explant body (Figure 6c).

3. Discussion

Recently, we established a toolbox of silk biomaterial scaffolds for neural tissue engineering that includes peripheral nerve guide conduits,[19,80,81] thin films for conformational electronics,[82] aligned electrospun nanofibers,[83] and porous aligned channel arrays.[84] The addition of silk hydrogels to our repertoire of neural tissue engineering scaffolds provides soft substrates to match nervous system tissue stiffness.

For successful application in nerve regeneration soft biomaterials must exhibit structural integrity and promote neurite extension by providing a mechanically and biochemically permissive environment. In the current studies, we found that silk hydrogels degrade slowly over several weeks to months, which would allow sufficient time for repair of significant nerve damage if employed in vivo. Furthermore, as previously studied, bioactivity of loaded morphogens was also maintained past 2 weeks. Other soft materials employed for studying effects of substrate stiffness on neuronal extension such as fibrin,[49] agarose,[48] and PDMS[42] can be tuned to achieve stiffness comparable to that of nervous tissue, but are often hindered by fast degradation (or melting) or cell toxicity. The present studies also found increased neurite extension as compared to reported values of those cultured on materials of similar stiffness. Man et al. studied the differences in DRG neurite extension in fibrin gels of 9.5–141 mg mL^{-1} protein yielding compressive moduli ranging from <5–80 kPa.[49] Interestingly, the length of neurite extension at 4 days was less when compared to silk hydrogels, ≈100–230 μm on fibrin versus over 1 mm on 1–2% silk hydrogels.[49]

It is interesting to note that although elastic moduli of the 1–8% w/v silk gels were within the reported ranges of neural cells and tissues, there was a significant difference in neurite growth rate observed. This phenomenon is likely due to a combination of factors resulting from the physical properties of the substrate, as well as the biological response of the cells. For example, it has been shown that in some cell types, integrins/cell adhesion molecules (i.e., β1 integrins and neural cell adhesion molecules in neurons) work in collaboration with growth factor receptors (i.e., TrkB/C in the case of NT-3) resulting in amplification of signaling pathways (i.e. Ras-Raf-Erk signaling necessary for neurotrophin-triggered axon elongation).[85–87] Therefore, in the case of neuronal growth on silk gels, it is possible that softer, lower percentage protein gels result in greater growth factor release, less growth factor immobilization, and lower integrin expression. In contrast, slightly stiffer gels of higher protein content may exhibit sufficient mechanical properties for optimal integrin expression as well as increased access to growth factors. Our observations of decreased neurite outgrowth on 8% vs. 4% silk gels suggests this hypothesis applies to a limited range of gel protein concentration, which may reach a point of diminishing returns (i.e., less or equivalent presentation of growth factor on the surface of 8% vs. 4% silk gels, Figure 4c). Others have also observed increased neurite extension on medium vs. softer or stiffer substrates.[31,49,88] Preliminary studies of increased β-1 integrin and TrkC expression of cDRGs cultured on 4% vs. 1% silk gels support this hypothesis.

Increased localization of growth factors to injury sites is also critical for neural regeneration. Studies by the Sakiyama-Elbert group have shown improved regeneration and functional recovery in 13 mm critical nerve defects with a fibrin affinity-based growth factor delivery system.[89–91] Studies have shown that 50–100% of growth factors are released from collagen[92] and fibrin[93–95] within 5–10 days. The current results show that only ≈5% NT-3 is released from 4% silk gels over 25 days (Figure 5) with the remaining growth factor promoting neurite extension after 11 days of release (Figure 4). Increased retention of growth factors and slow degradation properties of silk hydrogels (Figure 2) in addition to its soft mechanical properties offer favorable physical and biochemical properties as a biomaterial for nervous system applications.

Due to the increased durability in culture and prolonged degradation of silk hydrogels when compared to other natural

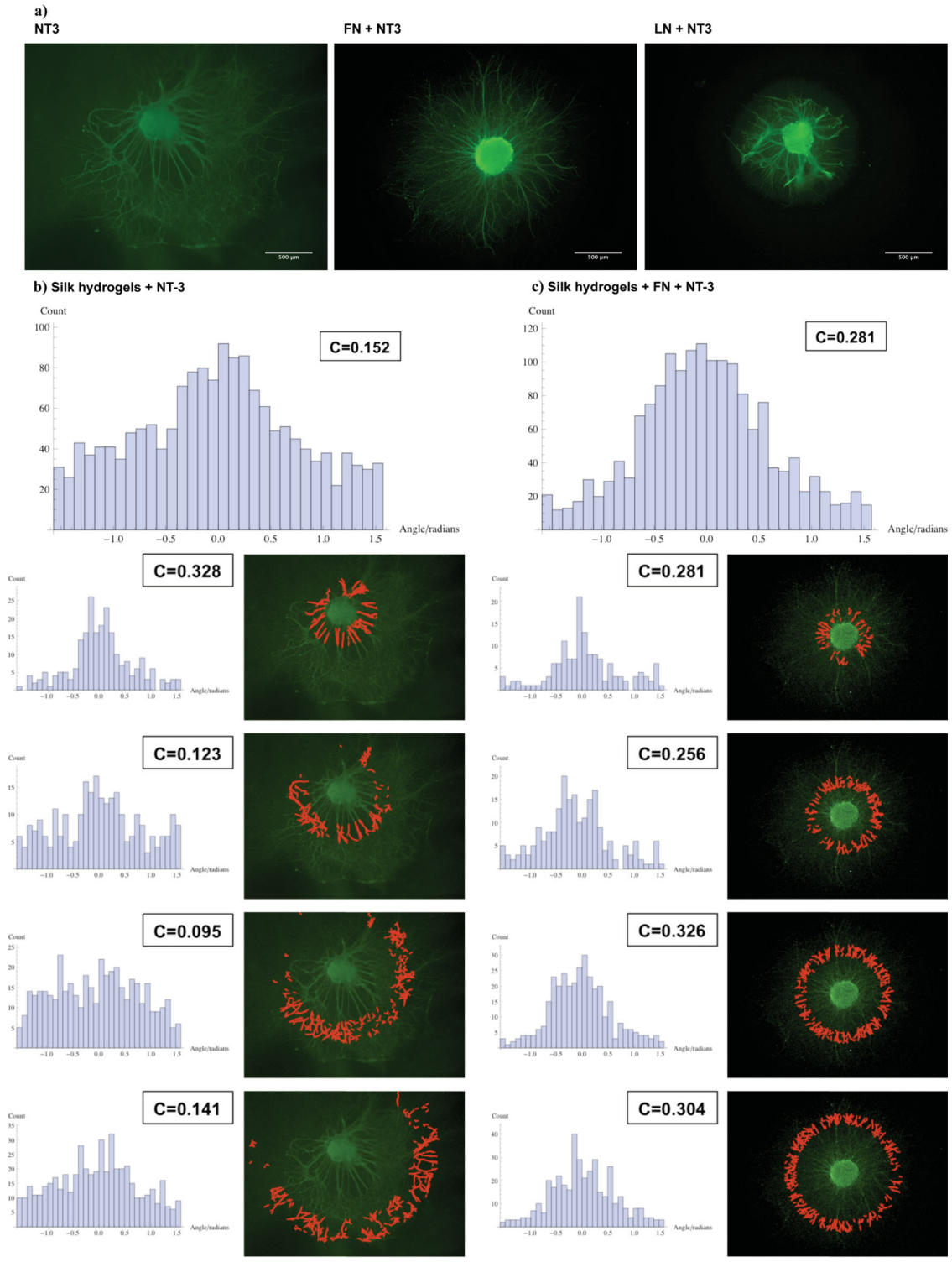

Figure 6. Neurite directional distribution analysis of cDRG neurite extension on silk hydrogels functionalized with ECM proteins. a) Representative cDRGs at day 4 in vitro on silk hydrogels loaded with NT-3 without ECM proteins, FN, or LN (L to R). b,c) Histogram and output images of neurite directional distribution analysis for cDRG neurite extension on silk hydrogels with b) 40 ng mL^{-1} NT-3 and c) NT-3 + FN. Quantitative results are given as 'C' values representing the first coefficient of the Fourier series expansion.

biomaterials, they are attractive candidates for the study of traction forces and axonal bundling on soft substrates that would otherwise lead to physical destruction of weaker gels. The physical mechanisms of growth cone guidance are beginning to be elucidated with recent findings showing that traction forces generated by DRG growth cones are significantly larger than those generated by hippocampal growth cones, which may be due to differences in cytoskeletal dynamics when navigating on substrates of different stiffness.[31,96] The current study yielded significant differences in the presence and spatial dependence of axonal fasciculation between substrates functionalized with and without FN (Figure 6). Neuronal fasciculation (axon bundling) occurs through contact attraction mediated by cell adhesion molecules present on axons.[97–99] It is still in question whether axons come together due to random movement of individual axons, repulsive and attractive signals from neighboring cells/neurites, or traction-like forces exerted by filopodia on each other.[99] Due to the presence of promiscuous integrin (in FN $III_{9\text{-}10}$) and growth factor (in FN $III_{12–14}$) binding sites on FN, increased axonal attachment and growth factor binding to silk hydrogels functionalized with FN + NT-3 would be expected on gels with FN versus those without.[39,40,100] Our observations of increased fasciculation in the presence of FN support the hypothesis that a multitude of physical mechanisms (i.e. increased integrin binding) and biochemical mechanisms (i.e. increased growth factor binding) contribute to increased overall neurite outgrowth as well as axonal fasciculation.

In conjunction with previous data on silk as a biomaterial,[52] the present studies reveal the attractive features of silk scaffolds for tissue engineering and regeneration. Not only is silk biocompatible and processed entirely under aqueous conditions, the versatility of available formats provides an extensive platform of architectural designs to accommodate every tissue in the body ranging from solid scaffolds to porous sponges to electrospun mats to hydrogels.[101] Furthermore, its stability and optical transparency despite its large molecular weight, natural source, and extensive range of stiffness render silk favorable for long-term culture and analysis of engineered ECMs and biologics. Together, this work contributes to previously reported features of silk scaffolds and suggests silk hydrogels for mediating the mechanical properties and ECM composition of engineered tissues.

4. Conclusions

The present work characterizes silk hydrogels as attractive candidates for neural tissue engineering with regards to stiffness compatibility, permissive environment for neuronal extension, ability to retain growth factors, and structural integrity for long-term growth studies. The silk hydrogel platform is also suitable for prolonged in vitro studies of the effects of substrate stiffness on neuronal extension and physiology by providing an in vivo-like mechanical environment for investigation of physiological mechanisms such as axonal fasciculation. These tools have significant potential for gaining a better understanding of how biomaterial substrates can be engineered and tailored for neural regeneration.

5. Experimental Section

Formation of Silk Hydrogels: Silk fibroin hydrogels were formed through ultrasonication of aqueous silk solution extracted from *Bombyx mori* silkworm cocoons as previously described.[52,102] Briefly, aqueous silk fibroin solutions were prepared by degumming cocoons in an alkaline solution of sodium carbonate (0.02 M) and rinsing thoroughly with ultrapure water. The fibers were dried overnight and then dissolved in LiBr (9.3 M) at 60 °C for 4 h. The silk protein solution was then purified by dialysis (Slide-A-Lyzer Dialysis Cassettes, 3.5K MWCO, 66333, Thermo Scientific, Rockford, IL) against distilled water for 48 h to obtain a 6–8% w/v silk solution. Silk solutions were prepared for hydrogel formation by diluting with 10× DMEM (Dulbecco's Modified Eagle Medium, Gibco, 12100-046) and dH_2O to obtain desired silk concentrations and 1× DMEM. To concentrate silk solution, dialysis against PEG (15%, 10 000 g mol^{-1}) was employed. The silk solution was filtered through 5 µm filters (Millex-SV, Millipore, SLSV025LS) before ultrasonication using a Branson sonifier (Branson Ultrasonics, Danbury, CT). Silk was sonicated at 20% maximum amplitude in 2 mL volumes and sonication times varied depending on silk concentration: 1, 2, 3, and 4 × 20 s for 1, 2, 4, and 8% w/v silk solutions, respectively. Gelation occurred within 2 h at 37 °C and remained at 37 °C overnight prior to experimentation (see below). For further characterization of silk hydrogel gelation and morphology, readers are directed to earlier works of Kim et al. and Hu et al.[54,55]

AFM Measurements: Silk hydrogels for AFM testing were prepared on glass surfaces as described above and incubated at 37 °C overnight. The next day, samples were submerged in Phosphate Buffered Saline (PBS) and equilibrated to room temperature. AFM testing was performed in PBS at room temperature and all samples were tested within 24 h. AFM force vs. indentation maps were acquired on an Asylum Research MFP3D AFM (Santa Barbara, CA) using Bruker tipless cantilevers (Camarillo, CA) with attached 6 µm radius silicone oxide microspheres (Corpuscular, Cold Spring, NY) and a spring constant of 0.112 N m^{-1}. Cantilevers were calibrated initially in air to determine the specific spring constant and then an additional calibration was performed after submersion in PBS to adjust for changes due to the liquid environment. Igor Pro (WaveMetrics, Inc., Lake Oswego, OR) software was used to obtain elastic modulus values from force vs indentation curves of points taken in a square grid of 2 µm spacing (n = 100 per grid).

Chick Dorsal Root Ganglion (cDRG) Culture: Silk hydrogels were formed as described above and loaded with or without NT-3, FN, and/or LN after sonication and prior to gelation. Fibrin gels (10 mg mL^{-1}) were fabricated by crosslinking fibrinogen (EMD Millipore, Darmstadt, Germany, 341578) with thrombin (Sigma-Aldrich, T6884) and collagen (BD Biosciences, 354236) gels (3-4 mg mL^{-1}) were formed by initiating crosslinking with increase in pH from NaOH at room temperature. cDRGs were isolated from E8-9 chick embryos as previously reported by Dichter and Fishbach and in accordance to Tufts IACUC regulations.[103] cDRGs were removed from either side of the spinal column and stored in HBSS (Hank's buffered saline solution, Gibco, 14170120) supplemented with dextrose (6 mg mL^{-1}) and $NaHCO_3$ (0.35 mg mL^{-1}) for up to 3 h until seeding. Excess tissue and residual roots were cleaned prior to seeding on hydrogels. Explants were allowed to attach for 1 h prior to addition of media (2% FBS DMEM, Glutamax, high glucose, (-) sodium pyruvate, 1% PenStrep). cDRGs were cultured on hydrogels for 4 days prior to 10% formalin fixation and immunostaining. For timelapse experiments, samples were fixed at each time point, immunostained and imaged at completion of the study.

Immunostaining and Fluorescent Imaging: After fixation overnight with 10% formalin, samples were washed with PBS, blocked with 4% normal goat serum (NGS, Sigma-Aldrich, G9023), permeabilized with 0.1% Triton X-100 (Sigma-Aldrich, X100), and incubated with anti-ß-tubulin III primary antibody produced in rabbit (Sigma-Aldrich, T2200) at 4 °C overnight. The next day, samples were washed 2-3× for 10–15 min while shaking before staining with Alexa Fluor 488 goat anti-rabbit IgG (Invitrogen, A-11008) shaking at room temperature for 40 min. Samples were again washed thoroughly with PBS prior to imaging.

Neurite Extension Analysis in ImageJ: Fluorescence microscopy images of cDRG explant cultures on silk hydrogels were analyzed using ImageJ software (National Institutes of Health, Bethesda, MD). Length was quantified using the segmented line tool and measure function. This tool allows manual tracing of neurites analagous to summing tangent vectors along the length of the neurite. After a completed tracing, the length of the segmented line was calculated and used as one measurement to represent outgrowth of the DRG. Eight random neurites were measured per explant, preferably 2 per quadrant of field of view. Percent area (of intensity) was also calculated to obtain a general quantification of neurite density. Circular selections were made within each quadrant of the image encompassing neurite extension from the outer edge of the explant body to neurite ends. $N \geq 4$ cDRGs per condition with multiple neurites (as described above) were measured per cDRG. Only neurites in focus with unambiguous extensions were recorded and explants that did not attach were discounted. Lengths were tabulated, statistics were applied, and values were compared across conditions. Significance of differences in neurite density and length was determined by Student's t-test in GraphPad Prism (La Jolla, CA) software.

Hydrogel Degradation Measurements: Silk, collagen, and fibrin hydrogels were formed as described above in pre-massed petri dishes. Masses of gels before degradation were recorded and gels were incubated in either Tris-$CaCl_2$ buffer alone or with enzyme (1.25 U α-chymotrypsin (Sigma-Aldrich, C3142) per 250 mg hydrogel). Masses were recorded day 1 and 3 and every 3 days thereafter. Degradation over time was reported in terms of percentage of original gel mass. Masses occasionally increased due to proposed increased hydration.

Growth Factor Release Studies: Silk hydrogels (4%, 300 μL) were formed in the wells of 12-well plates as outlined above except loaded with NT-3 (100 ng mL^{-1} Peprotech, 450-03) with or without FN (2 μM, Sigma-Aldrich, F2006). Molecules were loaded homogeneously by pipetting up and down appropriate amount of concentrated stock solution into silk solution after sonication, prior to gelation. Release was performed in release buffer of 0.1% BSA in PBS and samples were collected into 12-well plates pre-blocked with 1% BSA in PBS at regular time points. Cumulative release of NT-3 was quantified using Duoset ELISA (R&D Systems, DY267). Student's t-test was performed to determine significant differences between release profiles.

Bioactivity of NT-3 Loaded Silk Gels over 2 Weeks: Four percent w/v silk hydrogels were formed as described above, loaded with NT-3 (40 ng mL^{-1}), and incubated in cell culture medium for 1 or 11 days. Gels were then employed as substrates for cDRGs and analyzed by β-tubulin III immunofluorescent imaging as described above.

NT-3 Binding Assay: Silk hydrogels were formed as outlined above and fibrin gels were formed by mixing fibrinogen (10 mg mL^{-1}, EMD Millipore, Darmstadt, Germany, 341578) with thrombin (5 U mL^{-1}, Sigma-Aldrich, T6884). The gels were incubated in a solution of NT-3 (10 ng mL^{-1}) in 0.1% BSA in PBS overnight at 37 °C. TCP wells were also included as a positive controls. Negative control gel samples were incubated in 0.1% BSA in PBS without NT-3. The gels were then washed with PBS + 0.1% Tween 20 (PBS-Tween, Sigma-Aldrich, P1379), blocked with 1% BSA, and subjected to surface detection of NT-3 using a modified ELISA procedure. Briefly, the gels were incubated with biotinylated goat anti-human NT-3 (200 ng mL^{-1}, R&D Systems, 840211) for 1 h at room temperature and washed thoroughly with PBS-Tween. This was followed by incubation with Streptavidin-HRP (R&D Systems, 890803), thorough washing with PBS-Tween, and colorimetric quantification by incubation with Substrate Solution (1:1 H_2O_2:tetramethylbenzidine, R&D Systems, DY999). The reaction was stopped with 2N H_2SO_4 and the absorbance reading at 450 nm was measured with a SpectraMax M2 Microplate Reader (Molecular Devices, Sunnyvale, CA). Statistical significance was determined by one-way ANOVA in GraphPad Prism (La Jolla, CA).

Neurite Directional Distribution Analysis in Mathematica: Fasciculation of cDRG neurite extensions was assessed through a radial tangent vector profile analysis program.[79] Briefly, tangent lines were fit to continuous lines of fluorescence in immunofluorescent images of cDRG extension at day 4 of culture. The ODF of tangent vectors measured relative to the radially outward direction was computed both for the ensemble of neurites emanating from each explant and also for neurite sections within a sequence of concentric annuli centered around the explant body. The widths of these distribution functions and their variation between each annulus quantify the degree of fasciculation and its spatial dependence. 'C' values represent the coefficient of the first cosine term in the Fourier series expansion of the ODF providing quantification of the radially-oriented outgrowth of DRG neurites.

Statistics: GraphPad Prism software (La Jolla, CA) was employed for graphing and statistical analyses as stated above.

Acknowledgements

We would like to thank the IIE International Whitaker Program, the Laboratory for Regenerative Medicine and Pharmacobiology (LMRP) at EPFL, the NSF (CBET 1067093), the NIH (EB002520) and AFIRM for support of this work. We would specifically like to thank LMRP for contributions to the cDRG work and Brandon Wheeler and Courtney Connelly for participation in the degradation measurements.

Received: February 2, 2013
Published online: April 18, 2013

[1] N. C. f. I. P. a. C. Centers for Disease Control and Prevention, in *Injury Prevention & Control*, Vol. **2012**, Atlanta 2012.
[2] M. Ishihara, N. Mochizuki-Oda, K. Iwatsuki, H. Kishima, Y. Iwamoto, Y.-Ii. Ohnishi, M. Umegaki, T. Yoshimine, *J. Neurosci. Methods* **2011**, *198*, 181.
[3] R. D. Gurgo, K. S. Bedi, V. Nurcombe, *J. Clin. Neurosci.* **2002**, *9*, 613.
[4] J. Viventi, D. H. Kim, L. Vigeland, E. S. Frechette, J. A. Blanco, Y. S. Kim, A. E. Avrin, V. R. Tiruvadi, S. W. Hwang, A. C. Vanleer, D. F. Wulsin, K. Davis, C. E. Gelber, L. Palmer, J. Van der Spiegel, J. Wu, J. L. Xiao, Y. G. Huang, D. Contreras, J. A. Rogers, B. Litt, *Nat. Neurosci.* **2011**, *14*, 1599.
[5] A. A. Fomani, R. R. Mansour, *Sens. Actuators A* **2011**, *168*, 233.
[6] V. S. Polikov, P. A. Tresco, W. M. Reichert, *J. Neurosci. Methods* **2005**, *148*, 1.
[7] H. Lee, R. V. Bellamkonda, W. Sun, M. E. Levenston, *J. Neural Eng.* **2005**, *2*, 81.
[8] E. M. Pritchard, C. Szybala, D. Boison, D. L. Kaplan, *J. Controlled Release* **2010**, *144*, 159.
[9] Y. Zhong, R. V. Bellamkonda, *Brain Res.* **2007**, *1148*, 15.
[10] A. Mercanzini, S. Reddy, D. Velluto, P. Colin, A. Maillard, J.-C. Bensadoun, A. Bertsch, J. A. Hubbell, P. Renaud, *Proc. Ann. Int. I.E.E.E. E.M.B.S.* **2007**, 6613.
[11] A. H. Taub, R. Hogri, A. Magal, M. Mintz, Y. Shacham-Diamand, *J. Biomed. Mater. Res. A* **2012**, *100A*, 1854.
[12] X. Luo, C. L. Weaver, D. D. Zhou, R. Greenberg, X. T. Cui, *Biomaterials* **2011**, *32*, 5551.
[13] E. Azemi, C. F. Lagenaur, X. T. Cui, *Biomaterials* **2011**, *32*, 681.
[14] C. E. Schmidt, J. B. Leach, *Annu. Rev. Biomed. Eng.* **2003**, *5*, 293.
[15] J. Cao, C. Sun, H. Zhao, Z. Xiao, B. Chen, J. Gao, T. Zheng, W. Wu, S. Wu, J. Wang, J. Dai, *Biomaterials* **2011**, *32*, 3939.
[16] M. Lietz, L. Dreesmann, M. Hoss, S. Oberhoffner, B. Schlosshauer, *Biomaterials* **2006**, *27*, 1425.
[17] K. Jansen, J. F. A. van der Werff, P. B. van Wachem, J. P. A. Nicolai, L. de Leij, M. J. A. van Luyn, *Biomaterials* **2004**, *25*, 483.
[18] L. E. Kokai, A. M. Ghaznavi, K. G. Marra, *Biomaterials* **2010**, *31*, 2313.
[19] A. M. Ghaznavi, L. E. Kokai, M. L. Lovett, D. L. Kaplan, K. G. Marra, *Ann. Plast. Surg.* **2011**, *66*, 273.

[20] L. De Laporte, A. des Rieux, H. M. Tuinstra, M. L. Zelivyanskaya, N. M. De Clerck, A. A. Postnov, V. Preat, L. D. Shea, *J. Biomed. Mater. Res. A* **2011**, *98A*, 372.
[21] L. De Laporte, A. Huang, M. M. Ducommun, M. L. Zelivyanska, M. O. Aviles, A. F. Adler, L. D. Shea, *Acta Biomater.* **2010**, *6*, 2889.
[22] L. De Laporte, A. L. Yan, L. D. Shea, *Biomaterials* **2009**, *30*, 2361.
[23] D. M. Snow, E. M. Brown, P. C. Letourneau, *Int. J. Dev. Neurosci.* **1996**, *14*, 331.
[24] M. E. Bilozur, E. D. Hay, *Dev. Biol.* **1988**, *125*, 19.
[25] P. Singh, C. Carraher, J. E. Schwarzbauer, in *Annu. Rev. Cell Dev. Biol.*, Vol. *26* (Eds: R. Schekman, L. Goldstein, R. Lehmann), *Annual Reviews*, Palo Alto **2010**, 397.
[26] S. Sakashita, E. Engvall, E. Ruoslahti, *FEBS Lett.* **1980**, *116*, 243.
[27] B. S. Elkin, E. U. Azeloglu, K. D. Costa, B. Morrison, *J. Neurotrauma* **2007**, *24*, 812.
[28] Y. B. Lu, K. Franze, G. Seifert, C. Steinhauser, F. Kirchhoff, H. Wolburg, J. Guck, P. Janmey, E. Q. Wei, J. Kas, A. Reichenbach, *Proc. Natl. Acad. Sci. USA* **2006**, *103*, 17759.
[29] G.-L. Chang, T.-K. Hung, W. W. Feng, *J. Biomech. Eng.* **1988**, *110*.
[30] I. Levental, P. C. Georges, P. A. Janmey, *Soft Matter* **2007**, *3*, 299.
[31] D. Koch, W. J. Rosoff, J. Jiang, H. M. Geller, J. S. Urbach, *Biophys. J.* **2012**, *102*, 452.
[32] A. Kostic, J. Sap, M. P. Sheetz, *J. Cell Sci.* **2007**, *120*, 3895.
[33] J. S. Belkas, M. S. Shoichet, R. Midha, *Oper. Tech. Orthop.* **2004**, 190.
[34] B. J. Dickson, *Science* **2002**, *298*, 1959.
[35] S. D. Sanford, J. C. Gatlin, T. Hokfelt, K. H. Pfenninger, *Eur. J. Neurosci.* **2008**, *28*, 268.
[36] A. Hari, B. Djohar, T. Skutella, S. Montazeri, *Int. J. Dev. Neurosci.* **2004**, *22*, 113.
[37] C. Deister, S. Aljabari, C. E. Schmidt, *J. Biomater. Sci.-Polym. E.* **2007**, *18*, 983.
[38] J. B. Munson, D. L. Shelton, S. B. McMahon, *J. Neurosci.* **1997**, *17*, 470.
[39] S. Johansson, G. Svineng, K. Wennerberg, A. Armulik, L. Lohikangas, *Front. Biosci.* **1997**, *2*, D126.
[40] M. M. Martino, J. A. Hubbell, *FASEB J.* **2010**, *24*, 4711.
[41] Y. Luo, M. S. Shoichet, *Nat. Mater.* **2004**, *3*, 249.
[42] C.-M. Cheng, P. R. LeDuc, Y.-W. Lin, *J. Biomech.* **2011**, *44*, 856.
[43] L. L. Norman, H. Aranda-Espinoza, *Cell Mol. Bioeng.* **2010**, *3*, 398.
[44] L. A. Flanagan, Y. E. Ju, B. Marg, M. Osterfield, P. A. Janmey, *Neuroreport* **2002**, *13*, 2411.
[45] R. Mooney, S. Haeger, R. Lawal, M. Mason, N. Shrestha, A. Laperle, K. Bjugstad, M. Mahoney, *Tissue Eng. Part A* **2011**, *17*, 2805.
[46] I. Allodi, M.-S. Guzman-Lenis, J. Hernandez, X. Navarro, E. Udina, *J. Neurosci. Methods* **2011**, *198*, 53.
[47] J. P. Frampton, M. R. Hynd, M. L. Shuler, W. Shain, *Biomed. Mater.* **2011**, *6*, 015002.
[48] A. P. Balgude, X. Yu, A. Szymanski, R. V. Bellamkonda, *Biomaterials* **2001**, *22*, 1077.
[49] A. J. Man, H. E. Davis, A. Itoh, J. K. Leach, P. Bannerman, *Tissue Eng. Part A* **2011**, *17*, 2931.
[50] B. Panilaitis, G. H. Altman, J. S. Chen, H. J. Jin, V. Karageorgiou, D. L. Kaplan, *Biomaterials* **2003**, *24*, 3079.
[51] L. Meinel, S. Hofmann, V. Karageorgiou, C. Kirker-Head, J. McCool, G. Gronowicz, L. Zichner, R. Langer, G. Vunjak-Novakovic, D. L. Kaplan, *Biomaterials* **2005**, *26*, 147.
[52] C. Vepari, D. L. Kaplan, *Prog. Polym. Sci.* **2007**, *32*, 991.
[53] X. Hu, D. Kaplan, P. Cebe, *Macromolecules* **2008**, *41*, 3939.
[54] X. Hu, Q. Lu, L. Sun, P. Cebe, X. Wang, X. Zhang, D. L. Kaplan, *Biomacromolecules* **2010**, *11*, 3178.
[55] U. J. Kim, J. Y. Park, C. M. Li, H. J. Jin, R. Valluzzi, D. L. Kaplan, *Biomacromolecules* **2004**, *5*, 786.
[56] N. Guziewicz, A. Best, B. Perez-Ramirez, D. L. Kaplan, *Biomaterials* **2011**, *32*, 2642.
[57] O. Etienne, A. Schneider, J. A. Kluge, C. Bellemin-Laponnaz, C. Polidori, G. G. Leisk, D. L. Kaplan, J. A. Garlick, C. Egles, *J. Periodontol.* **2009**, *80*, 1852.
[58] J. A. Kluge, N. C. Rosiello, G. G. Leisk, D. L. Kaplan, A. L. Dorfmann, *J. Mech. Behav. Biomed. Mater.* **2010**, *3*, 278.
[59] K. M. Lorentz, S. Kontos, P. Frey, J. A. Hubbell, *Biomaterials* **2011**, *32*, 430.
[60] S. Liao, F. Watari, Y. Zhu, M. Uo, T. Akasaka, W. Wang, G. Xu, F. Cui, *Dent. Mater.* **2007**, *23*, 1120.
[61] T. D. Gordon, L. Schloesser, D. E. Humphries, M. Spector, *Tissue Eng.* **2004**, *10*, 1287.
[62] T. Wen, J. H. Gong, Z. J. Peng, D. Y. Jiang, C. B. Wang, Z. Q. Fu, H. Z. Miao, *Mater. Chem. Phys.* **2011**, *125*, 500.
[63] J. Y. Rho, R. B. Ashman, C. H. Turner, *J. Biomech.* **1993**, *26*, 111.
[64] Y. P. Zheng, A. F. T. Mak, *P. Ann. Int. I.E.E.E. E.M.B.S.* **1997**, *19*, 2246.
[65] J. B. Scott, M. Afshari, R. Kotek, J. M. Saul, *Biomaterials* **2011**, *32*, 4830.
[66] M. Ahearne, K. K. Liu, A. J. El Haj, K. Y. Then, S. Rauz, Y. Yang, *Tissue Eng. Part C-Methods* **2010**, *16*, 319.
[67] M. Ahearne, Y. Yang, A. J. El Haj, K. Y. Then, K. K. Liu, *J. R. Soc. Interface* **2005**, *2*, 455.
[68] A. Conovaloff, A. Panitch, *J. Neural Eng.* **2011**, *8*, 056003.
[69] L. Fang, Y.-N. Wang, X.-L. Cui, S.-Y. Fang, J.-Y. Ge, Y. Sun, Z.-H. Liu, *J. Cell Sci.* **2012**, *125*, 1500.
[70] Z. Fanti, M. Elena Martinez-Perez, F. F. De-Miguel, *Dev. Neurobiol.* **2011**, *71*, 870.
[71] M. Schwartz, N. Spirman, *Proc. Natl. Acad. Sci. USA* **1982**, *79*, 6080.
[72] S. Madduri, M. Papaloizos, B. Gander, *Biomaterials* **2010**, *31*, 2323.
[73] H. B. Wang, M. E. Mullins, J. M. Cregg, C. W. McCarthy, R. J. Gilbert, *Acta Biomater.* **2010**, *6*, 2970.
[74] E. Schnell, K. Klinkhammer, S. Balzer, G. Brook, D. Klee, P. Dalton, J. Mey, *Biomaterials* **2007**, *28*, 3012.
[75] T. Freier, R. Montenegro, H. S. Koh, M. S. Shoichet, *Biomaterials* **2005**, *26*, 4624.
[76] T. T. Yu, M. S. Shoichet, *Biomaterials* **2005**, *26*, 1507.
[77] W. J. Zhang, X. L. Wang, S. Y. Wang, J. Zhao, L. Y. Xu, C. Zhu, D. L. Zeng, J. Chen, Z. Y. Zhang, D. L. Kaplan, X. Q. Jiang, *Biomaterials* **2011**, *32*, 9415.
[78] T. B. Kuhn, M. F. Schmidt, S. B. Kater, *Neuron* **1995**, *14*, 275.
[79] A. M. Hopkins, B. Wheeler, C. Staii, D. L. Kaplan, T. J. Atherton, *unpublished*.
[80] A. R. Nectow, K. G. Marra, D. L. Kaplan, *Tissue Eng. Part B-Rev.* **2012**, *18*, 40.
[81] Y.-C. Lin, M. Ramadan, M. Hronik-Tupaj, D. L. Kaplan, B. J. Philips, W. Sivak, J. P. Rubin, K. G. Marra, *Ann. Plast. Surg.* **2011**, *67*, 147.
[82] D.-H. Kim, J. Viventi, J. J. Amsden, J. Xiao, L. Vigeland, Y.-S. Kim, J. A. Blanco, B. Panilaitis, E. S. Frechette, D. Contreras, D. L. Kaplan, F. G. Omenetto, Y. Huang, K.-C. Hwang, M. R. Zakin, B. Litt, J. A. Rogers, *Nat. Mater.* **2010**, *9*, 511.
[83] C. R. Wittmer, T. Claudepierre, M. Reber, P. Wiedemann, J. A. Garlick, D. Kaplan, C. Egles, *Adv. Funct. Mater.* **2011**, *21*, 4232.
[84] Q. Zhang, Y. Zhao, Y. Shuqin, Y. Yang, H. Zhao, M. Li, S. Lu, D. Kaplan, *Acta Biomater.* **2012**, *8*, 2628.
[85] A. Markus, T. D. Patel, W. D. Snider, *Curr. Opin. Neurobiol.* **2002**, *12*, 523.
[86] K. R. Legate, S. A. Wickstroem, R. Faessler, *Genes Dev.* **2009**, *23*, 397.
[87] J. Ivaska, J. Heino, *Annu. Rev. Cell Dev. Biol.* **2011**, *27*, 291.
[88] K. J. Lampe, A. L. Antaris, S. C. Heilshorn, *Acta Biomater.* **2012**, *9*, 5590.

[89] M. D. Wood, M. R. MacEwan, A. R. French, A. M. Moore, D. A. Hunter, S. E. Mackinnon, D. W. Moran, G. H. Borschel, S. E. Sakiyama-Elbert, *Biotechnol. Bioeng.* **2010**, *106*, 970.
[90] M. D. Wood, D. Hunter, S. E. Mackinnon, S. E. Sakiyama-Elbert, *J. Biomater. Sci.-Polym. E.* **2010**, *21*, 771.
[91] M. D. Wood, A. M. Moore, D. A. Hunter, S. Tuffaha, G. H. Borschel, S. E. Mackinnon, S. E. Sakiyama-Elbert, *Acta Biomater.* **2009**, *5*, 959.
[92] J. M. Wu, Y. Y. Xu, Z. H. Li, X. Y. Yuan, P. F. Wang, X. Z. Zhang, Y. Q. Liu, J. Guan, Y. Guo, R. X. Li, H. Zhang, *J. Mater. Sci. Mater. Med.* **2011**, *22*, 107.
[93] C. T. Drinnan, G. Zhang, M. A. Alexander, A. S. Pulido, L. J. Suggs, *J. Controlled Release* **2010**, *147*, 180.
[94] S. E. Sakiyama-Elbert, J. A. Hubbell, *J. Controlled Release* **2000**, *69*, 149.
[95] M. D. Wood, G. H. Borschel, S. E. Sakiyama-Elbert, *J. Biomed. Mater. Res. Part A* **2009**, *89A*, 909.
[96] E. Spedden, J. D. White, D. Kaplan, C. Staii, *MRS Online P. Libr.* **2012**, 1420.
[97] J. Dodd, T. M. Jessell, *Science* **1988**, *242*, 692.
[98] H. O. Nornes, G. D. Das, *Proc. Natl. Acad. Sci. USA* **1972**, *69*, 1962.
[99] H. G. E. Hentschel, A. van Ooyen, *Physica A* **2000**, *288*, 369.
[100] M. M. Martino, F. Tortelli, M. Mochizuki, S. Traub, D. Ben-David, G. A. Kuhn, R. Mueller, E. Livne, S. A. Eming, J. A. Hubbell, *Sci. Transl. Med.* **2011**, *3*, 100ra89.
[101] D. N. Rockwood, R. C. Preda, T. Yucel, X. Wang, M. L. Lovett, D. L. Kaplan, *Nat. Protocols* **2011**, *6*, 1612.
[102] X. Q. Wang, J. A. Kluge, G. G. Leisk, D. L. Kaplan, *Biomaterials* **2008**, *29*, 1054.
[103] M. A. Dichter, G. D. Fischbach, *J. Physiol. (Lond.)* **1977**, *267*, 281.